Voyagaki, E., Crispin, J., Gilder, C., Nowak, P., O'Riordan, N., Patel, D., & Vardanega, P. (2019). Analytical Approaches to Predict Pile Settlement in London Clay. In H. El-Naggar, K. Abdel-Rahman, B. Fellenius, & H. Shehata (Eds.), *Sustainability Issues for the Deep Foundations: Proceedings of the 2nd GeoMEast International Congress and Exhibition on Sustainable Civil Infrastructures, Egypt 2018 – The Official International Congress of the Soil-Structure Interaction Group in Egypt (SSIGE)* (pp. 162-180). (Sustainable Civil Infrastructures). Springer, Cham. https://doi.org/10.1007/978-3-030-01902-0_14

Peer reviewed version

Analytical Approaches to Predict Pile Settlement in London Clay

Elia Voyagaki[1] PhD, Jamie Crispin[2] MEng, Charlotte Gilder[2] MSci, Paul Nowak[3] BSc, Nick O'Riordan[4] PhD, Dinesh Patel[5] MSc and Paul J Vardanega[6] PhD

[1] Research Associate, University of Bristol, Bristol, UK; e.voyagaki@bristol.ac.uk
[2] PhD student, University of Bristol, Bristol, UK
[3] Technical Director, Atkins, Epsom, UK
[4] Director and Arup Fellow, Arup, London, UK
[5] Director, Arup, London, UK
[6] Lecturer in Civil Engineering, University of Bristol, Bristol, UK

ABSTRACT: Projects involving construction of piled foundations often rely on preliminary full-scale field tests to failure to predict performance under applied load. If these tests are not available, the ensuing uncertainty will naturally lead to conservative design assumptions. Such design assumptions will result in higher construction costs and often in longer construction times. This paper shows how a database of previous pile load tests can be used in conjunction with simple analytical tools to attempt a quantification of performance uncertainty. Data from a series of previously published axial load tests on piles in London Clay is employed to this end. The methodology developed in this paper can arguably be expanded to a wider range of test sites and geological materials.

INTRODUCTION

Piled foundations 'fail' due to excessive movements. Literature on estimating the magnitude of these movements is extensive; ranging from analytical solutions (e.g., Randolph & Wroth 1978; Mylonakis & Gazetas 1998; Mylonakis 2001, Guo 2012), continuum solutions employing Green's functions (e.g., Poulos & Davis 1968, Butterfield & Banerjee 1971), finite-element studies (e.g., Ottaviani 1975; Baguelin & Frank 1980; Syngros 2004) and semi-empirical approaches (e.g., Seed & Reese 1957; Coyle & Reese 1966; and Fleming 1992). Despite these advances, engineers "may never be able to estimate axial pile capacity in many soil types more accurately than about ±30%" (Randolph 2003).

The significance of accessible open source data has been acknowledged by other researchers who have invested in databases of pile performance in various countries e.g., USA (Paikowsky *et al.* 2004), Ireland (Galbraith *et al.* 2014) and Egypt (AbdelSalam *et al.* 2015). Global databases have also been recently compiled for tests in sands by a Chinese-UK-Australian research collaboration (Yang *et al.* 2015, 2016) and the FindaPile.com (Lemnitzer & Favaretti 2013) database for lateral-load tests by the Deep Foundation Institute and University of California, Irvine in the USA.

In the UK, a large amount of piled foundation construction is in stiff clay deposits. Results of full-scale tests on bored piled foundations are available for London clay (Whitaker & Cooke 1966, Patel 1992), but the raw data is not widely available. Design methods used in practice include those reported in Skempton (1959) (see Figure 1a), Poulos (1989), Fleming *et al*. (2009) and Tomlinson & Woodward (2014).

Settlement prediction is often carried out using numerical software such as Oasys Pile (OASYS 2017), Ensoft TZPile (Reese *et al*. 2014), Geocentrix Repute (Bond & Basile 2017), Deltares D-Pile group (Deltares 2016) and Fine GEO5 Pile (Fine n.d.). The available software use either three-dimensional boundary element methods based on Mindlin's solution for a point load in the interior of a linear elastic half space, or one-dimensional numerical analysis using theoretical or empirical "*t-z*" curves.

Combining the load test data collected in the stiff clay deposits in the UK in the past is needed to better calibrate geotechnical design models and thus better quantify and hopefully reduce uncertainty. Such data are key for calibrating recent analysis models. This paper presents the preliminary outcomes of an EPSRC funded research project (DINGO: Databases to INterrogate Geotechnical Observations) for the development of an open-source database of pile load tests in UK soil deposits.

THE DATABASE: KEY FEATURES AND STRUCTURE

At the time of writing the DINGO database was being compiled by a research team based at the University of Bristol. Data from literature includes material published in journals, conference proceedings, textbooks, dissertations and technical reports. Industry data has been sourced from UK-based engineering consultancies and contractors.
The Association of Geotechnical & Geoenvironmental Specialists (AGS) present a data structure, known as the AGS Format (AGS 4.0.4, 2017), which is commonly used for transfer of ground investigation data in the UK. This was selected for the DINGO database to allow ease of use and familiarity to the practicing engineer. A similar structure is not available for pile loading tests, therefore, a similar but bespoke format has been used for the pile information. The source metadata is stored in a master spreadsheet with additional spreadsheets describing the site-specific data.

PRELIMINARY ANALYSIS AND RESULTS

Once the database of tests is compiled, the aim is to use it to calibrate and compare existing settlement prediction approaches available in the literature. In this paper a preliminary investigation focuses into suitable methods to use and the appropriate presentation methods to allow comparison between them. A large number of prediction methods are available both in the literature and in software packages as mentioned in the Introduction. Three families of methods are considered and a representative model is chosen from each.

Method 1 – Linear Elastic

Linear elastic analyses are commonly used to model piles under axial load. Some software still exclusively uses linear elastic soil models (e.g. PIGLET, Randolph 2006) and most software includes an option to use this model. Simplified Winkler/load transfer models are popular (Randolph & Wroth, 1978; Scott, 1981; Mylonakis & Gazetas 1998; Guo 2012), and when model parameters are matched to soil properties using more rigorous continuum analyses that typically provide very similar results (Randolph & Wroth, 1978; Mylonakis, 2001; Syngros, 2004; Guo, 2012; Anoyatis, 2013). Closed-form solutions for piles embedded in inhomogeneous soils are provided, among others, by Scott (1981), Guo (2012) and Crispin *et al*. (2018). The method by Crispin *et al.* (2018) has been chosen to represent this 'family' of solutions, in which the Winkler model is employed, and the Winkler modulus is assumed to vary according to the following function of depth, z:

$$k(z) = k_L \left[a + (1-a)\frac{z}{L} \right]^n, \quad a = \left(\frac{k_0}{k_L} \right)^{\frac{1}{n}} \tag{1}$$

where L is the pile length, k_0 and k_L are the Winkler modulus at the pile head and pile base, respectively; a is a dimensionless coefficient accounting for non-zero surface stiffness and n is an inhomogeneity exponent. The pile base is modelled as a spring with stiffness K_b.

The pile head stiffness, K_0, is given by:

$$K_0 = E_p A \lambda_L a^{\frac{n}{2}} \frac{\left[I_{\nu-1}(\chi_0) I_{1-\nu}(\chi_L) - I_{1-\nu}(\chi_0) I_{\nu-1}(\chi_L) \right] + \Omega_L \left[I_{\nu-1}(\chi_0) I_{-\nu}(\chi_L) - I_{1-\nu}(\chi_0) I_{+\nu}(\chi_L) \right]}{\left[I_{-\nu}(\chi_0) I_{\nu-1}(\chi_L) - I_{+\nu}(\chi_0) I_{1-\nu}(\chi_L) \right] + \Omega_L \left[I_{-\nu}(\chi_0) I_{+\nu}(\chi_L) - I_{+\nu}(\chi_0) I_{-\nu}(\chi_L) \right]} \tag{2}$$

where E_p and A denote the pile elastic modulus and cross-sectional area, respectively; λ_L is a load transfer parameter (units of Length^{-1}); Ω_L a dimensionless pile base stiffness constant and $I_\nu(\chi)$ is the modified Bessel function of the first kind of order ν and argument χ. λ_L, Ω_L, ν, χ_L and χ_0 are given by:

$$\lambda_L = \sqrt{\frac{k_L}{E_p A}}, \ \Omega_L = \frac{K_b}{E_p A \lambda_L}, \ \nu = \frac{1}{n+2}, \ \chi_L = \frac{2\lambda_L L}{(1-a)(n+2)}, \ \chi_0 = \chi_L a^{\frac{n+2}{2}} \tag{3}$$

The Winkler modulus and base spring stiffness must then be related to the soil properties. The simple concentric cylinder model from Cooke (1974) and Randolph & Wroth (1978) (Figure 1b) is used to relate the Winkler modulus variation, $k(z)$, to the soil shear modulus variation, $G_s(z)$ by defining a "magical" radius, r_m, denoting the radial distance from the pile axis at which displacement due to the load applied on the pile is presumed to reach zero. For a single pile the stiffness of the springs in the shaft can be determined using the following expression (Randolph & Wroth 1978).

$$\frac{k(z)}{G_s(z)} \approx \frac{2\pi}{\ln(2r_m / D_s)}, \quad r_m \approx 2.5L\frac{G_s(L/2)}{G_s(L)}(1-\nu_S) \tag{4}$$

where D_s is the pile shaft diameter and ν_s is the soil Poisson's ratio. The expression for r_m was fitted to a numerical continuum analysis by Randolph & Wroth (1978).

Pile groups spaced closer than r_m (≈5-10D_s) are interacted and Poulos (1968) superposition method can be applied using the interaction factors of Randolph & Wroth (1979) as modified by Mylonakis & Gazetas (1998), to determine the overall settlement of the group.

The stiffness of the pile base spring, K_b, is approximated as a rigid punch on the surface of a half-space (Randolph & Wroth, 1978):

$$K_b \approx \frac{2G_s(L)D_b}{(1-\nu_s)} \tag{5}$$

where D_b is the pile base diameter.

Linear elastic models, including the herein presented method, are easy to employ with sufficient accuracy at low strength mobilisations which are often encountered in design. However, these methods do not account for the nonlinear behavior of the soil which can lead to very unconservative predictions at large loads, close to failure.

Method 2 – Elastoplastic "*t-z*" analysis using a linear elastic perfectly-plastic soil model

The simplest non-linear model is linear elastic-perfectly plastic, which is commonly the default for settlement prediction software (e.g. OASYS 2017; Deltares, 2016) and allows model parameters to be easily related to soil properties. A simple extension to the linear elastic model has been described by Scott (1981), Guo (2012) and Crispin *et al*. (2018) that allows this model to be analysed in closed form, without the need for numerical software. The analysis proposed by Crispin *et al.* (2018) is used in this study.

The model is shown in Figure 2. Following the assumption that the limiting skin friction is first reached at ground surface, and a plastic length, L_p, propagates down the pile, parametric expressions for the load and settlement at the top of the pile can be developed in terms of L_p. At the interface between this plastic section and the elastic section below, the displacement of the pile is the yield displacement at that depth, $w_y(L_p)=t_u(L_p)/k(L_p)$. The stiffness of the elastic section, K_{el}, can be calculated using any linear elastic method and multiplied by $w_y(L_p)$ to get the axial force in the pile at the interface. The plastic section of pile is then modelled as a column with known base load and distributed shaft load. Once the shaft resistance is exhausted, a displacement at the pile base can be assumed and the same process applied with the elastic section replaced by the base spring. By calculating the head load and settlement for $0 \leq L_p \leq L$ and for the base settlement at failure, a full load-settlement curve can be produced.

Considered a power-law variation in ultimate shaft resistance per unit length, $t_u(z)$, with exponent, m, and surface value t_{u0}, Crispin *et al.* (2018) developed Eqs (6) and (7) to describe the head load and settlement:

$$P = P(L_p) + t_{u0}L_p + \frac{t_u(L_p) - t_{u0}}{m+1} L_p \tag{6}$$

$$w_0 = w(L_p) + \frac{P(L_p)}{E_p A} L_p + \frac{t_{u0}}{2E_p A} L_p^{\ 2} + \frac{t_u(L_p) - t_{u0}}{(m+2)E_p A} L_p^{\ 2} \tag{7}$$

where $w(L_p)$, $P(L_p)$ and $t_u(L_p)$ are the axial displacement, load and ultimate shaft resistance per unit length at the interface depth, $z=L_p$, respectively.

$t_u(z)$ is calculated using the α-method (Skempton, 1959; Patel, 1992):

$$t_u(z) = \alpha c_u(z) \pi D_s \tag{8}$$

where α is the pile-soil adhesion factor and $c_u(z)$ is the undrained shear strength profile with depth.

This extension of the linear elastic method gives more reasonable predictions at large loads yet is simpler to employ than full numerical analysis, but careful consideration is therefore required to select a representative stiffness and strength (e.g. Poulos 1999).

Method 3 – Elastoplastic "*t-z*" analysis using a power–law nonlinear soil model
A linear elastic perfectly-plastic soil model is a relatively crude approximation of the constitutive behavior of soils, neglecting any nonlinear elastic behavior and plastic behavior such as strain softening. Modelling soil nonlinearity rigorously requires numerical analysis, however, Vardanega *et al.* (2012a, 2018) proposed a simple analytical method based on mobilised stress design principles that is suitable for hand calculation and can be applied here. The constitutive relationship in Eq. (9) was derived from a database of soil tests in clays (Vardanega & Bolton, 2011a).

$$\frac{1}{M} = \frac{\tau}{c_u} = \frac{1}{2}\left(\frac{\gamma}{\gamma_{M=2}}\right)^b \quad , \quad 1.25 \leq M \leq 5 \tag{9}$$

where M is the mobilisation factor, a factor of safety on soil shear strength c_u; τ is the mobilised shear stress at a corresponding shear strain γ; $\gamma_{M=2}$ is the shear strain at 50% of the undrained shear strength and b is a nonlinearity exponent.

By applying this relationship to the concentric cylinder model introduced by Cooke (1974) and Randolph & Wroth (1978) (Figure 1b) and accounting for pile compression, Vardanega *et al.* (2012a) derived the following relationship between the average mobilisation of soil strength at the pile circumference and the displacement at the pile head:

$$\frac{w_h}{D_s} = \frac{b \cdot \gamma_{M=2}}{2(1-b)} \left(\frac{2}{M} \right)^{1/b} + \frac{2}{M} \frac{\overline{c_u}}{E_p} \left(\frac{L}{D_s} \right)^2 \tag{10}$$

where $\overline{c_u}$ is the average undrained shear strength over the pile length.

In order to apply Eq. (10), a relationship between the applied load at the pile head and the mobilisation of the soil at the pile circumference is required. Using the adhesion factor α, on soil shear strength (Skempton, 1959; Patel, 1992) to estimate the shear stress at the pile-soil interface when slip occurs, the mobilisation factor can be related to the factor of safety on the pile shaft resistance, F_{shaft}:

$$F_{shaft} = \frac{P_{u,s}}{P_s} = \alpha M \tag{11}$$

where P_s and $P_{u,s}$ are the applied and ultimate load on the shaft, respectively and M is the average mobilisation factor over the pile length. This indicates that the minimum value of M is $1/\alpha$. Following the conservative simplifying assumption that no base load is mobilised until the shaft resistance is exhausted, the total factor of safety, F_{total}, is given by:

$$F_{total} \cong \frac{P_{u,s} + P_{u,b}}{P_s} = \frac{P_{u,s} + P_{u,b}}{P_{u,s}} F_{shaft} = \frac{P_{u,s} + P_{u,b}}{P_{u,s}} \alpha M \tag{12}$$

where $P_{u,b}$ is the ultimate load resisted by the pile base. Substituting the following expressions for $P_{u,s}$ and $P_{u,b}$ (Skempton, 1959) into Eq. (12) yields Eq. (14).

$$P_{u,s} = \alpha \overline{c_u} \pi D_s L \ , \ P_{u,b} = N_c c_{ub} \pi D_b^2 / 4 \tag{13}$$

$$F_{total} = \frac{P_u}{P} = \left[\alpha + \frac{N_c}{4} \frac{c_{ub}}{\overline{c_u}} \frac{D_s}{L} \left(\frac{D_b}{D_s} \right)^2 \right] M \tag{14}$$

where P and P_u are the total applied and ultimate loads, respectively; N_c is the bearing capacity factor, taken as 9, and c_{ub} is the undrained shear strength at the pile base.

The power-law constitutive model is an improvement on a linear elastic assumption and the method employed is still simple to apply. However, once the shaft resistance is exhausted, the concentric cylinder model no longer applies and Eq. (11) cannot be used, therefore this method is limited to predicting settlement before the shaft resistance is exhausted.

Analysis

The methods described in the previous sections have been used to analyse 51 maintained load tests from 15 sites in London reported by Patel (1989). A summary of the tests is shown in Tables 1 and 2. All piles are embedded in London Clay with a short, commonly sleeved, length through any overlying material.

Patel (1989) interpreted mean $c_u(z)$ lines for each site using triaxial test results, as is now recommended by the London District Surveyors Association (LDSA, 2009). Most of these lines were determined from undrained triaxial shear tests on 100*mm* samples, therefore, following the recommendations of Patel (1992) and LDSA (2009), $\alpha=0.5$ has been used directly from back analysis of reported maintained load pile test results. However, for sites A5, A7, A8 and A14 the design lines were based on c_u tests on 38*mm* samples. Patel (1992) found that 38*mm* samples overestimate the fissured strength of London Clay (found using plate load tests or using 100*mm* samples) by a factor of about 1.3, therefore, the design lines for these sites have been reduced by this factor. This is in agreement with experimental results by Whitaker & Cooke (1966) who used 38*mm* samples and recommended reducing the base value by a similar factor. The equivalent α value is 0.38, which is similar to the value found by Skempton (1959) using the approach after Patel (1992) to account for the slower rate at which these tests were completed. Skempton's work (1959) was largely based on very fast tests to failure at a time when rate and pore pressure effects in stiff clays were unknown. The design lines are shown in Figure 4.

Vardanega & Bolton (2011b) analysed 15 high quality triaxial tests on London Clay samples to determine the deformation behaviour of the material. The tests had an average b value of 0.58 and an average $\gamma_{M=2}$ of 7×10^{-3}, which are used in Method 3. Additionally, the maximum shear modulus, G_0, was found to be approximately $320c_u$. G_0 is used in Methods 1 and 2 until the shaft resistance is exhausted. A secant shear modulus is employed for the remaining settlement in Method 2, resulting in a bilinear spring to represent the base (shown in Figure 3a). This is estimated using Eq. (9) and the predicted mobilisation of the base resistance once the shaft resistance was exhausted and at failure (shown in Figure 3b).

Results

Load-settlement curves for each test are presented in Figures 5 to 7 comparing the three predicted curves with the measured data. The head displacement is normalised with the pile base diameter and the applied load is normalised with the predicted ultimate load using Eq. (13). This has been equated to the inverse of the design Factor of Safety (F_{total}). The predicted ultimate load for each pile is shown in Table 3 with the maximum load tested and the valid prediction range of each method. All three methods predict the settlement well at low loads, indicating the deformation parameters chosen are realistic. Method 1 under-predicts settlement significantly at high loads when nonlinear soil behaviour dominates. Method 2 accounts for this relatively well, although the linear elastic perfectly-plastic model provides a sharp transition to yielding. Method 3 shows good agreement over the range for which it is valid but should not be used beyond the point where the shaft resistance is exhausted.

The predicted and measured settlements at specific F_{total} values have been interpolated. Predicted versus measured plots are needed to show the bandwidth of error when using a model to predict observations (cf. Koutsoftas *et al.* 2017 and Kootahi & Mayne 2017). Figure 8 shows the predicted vs. measured settlement for each model at F_{total}=2.5. Vardanega *et al*. (2012b) shows that various codified design approaches for a pile in London Clay imply F_{total} values around this level while, LDSA (2009) recommends a value of 2.6 for piles in London Clay where no load testing is completed. 50% error bounds and the percentage of points within this range for each method are shown. Higher points indicate unconservative predictions. Figure 9 illustrates similar plots for F_{total} values of 5, 3, 2, and 1.5. These allow a designer to observe the possible variation in pile settlement predictions in London Clay at different factors of safety. The maintained load tests in the database studied here were not carried out to failure so the number of tests on the plot reduces as the applied load increases. All three models seem to initially give conservative predictions, however, as the F_{total} gets lower it is apparent that some results were significantly under-predicted.

CONCLUSIONS

An opensource, user-friendly database for UK pile tests is being compiled at the University of Bristol. Preliminary analyses were presented concerning the data from Patel's (1989) database of field tests. Experimental measurements were compared to three selected theoretical approaches from three groups: (i) linear elastic, (ii) elastoplastic "*t-z*" analysis using a linear elastic perfectly-plastic soil model, and (iii) elastoplastic "*t-z*" analysis using a power-law non-linear soil model. All three selected methods, although idealised, show good agreement with the test data. An alternative representation comparing predicted vs. measured normalised pile head settlement proves desirable, as it allows for a better understanding of the accuracy of the theoretical models in a statistical sense.

DATA AVAILABILITY STATEMENT

The work reported in this paper has not generated new experimental data.

ACKNOWLEDGMENTS

The authors acknowledge the support of University of Bristol and "Databases to INterrogate Geotechnical Observations (DINGO)" EP/P020933/1 EPSRC. The second and third authors were supported by the Engineering and Physical Sciences Research Council [grant numbers: EP/N509619/1 and EP/R51245X/1, respectively]. The authors would like to thank Professor George Mylonakis for his valuable support in

the preparation of this manuscript and Dr Melvin England for his helpful comments and suggestions.

REFERENCES

AbdelSalam, S.S., Baligh, F.A. and El-Naggar, H.M. (2015). A database to ensure reliability of bored pile design in Egypt. Proceedings of the Institution of Civil Engineers – Geotechnical Engineering, **168**(2), 131-143, https://doi.org/10.1680/geng.14.00051.

Anoyatis, G.M. (2013). Contribution to kinematic and inertial analysis of piles by analytical and experimental methods. Ph.D. thesis. University of Patras, Patras, Greece.

Association of Geotechnical and Geoenvironmental Specalists (AGS), (2017). Electronic Transfer of Geotechnical and Geoenvironmental Data, Edition 4.0.4. Bromley, Kent, UK.

Baguelin, F., and Frank, R. (1980). Theoretical studies of piles using the finite element method. In: Numerical Methods in Offshore Piling, Institution of Civil Engineers (ICE), London, 83-91.

Bond, A. and Basile, F. (2017) Geocentrix Repute 2.5 Reference Manual – Onshore pile design and analysis. Geocentrix Ltd. Available at: http://www.geocentrix.co.uk/repute/downloads/Repute%202.5%20Reference%20Manual.pdf, accessed 29th June 2018.

Butterfield, R. and Banerjee, P.K. (1971). The elastic analysis of compressible piles and pile groups. Géotechnique, **21**(1), 43-60, https://doi.org/10.1680/geot.1971.21.1.43.

Cooke, R. W. (1974). The settlement of friction pile foundations. In Proceedings of the Conference Tall Buildings, Kuala Lumpur, No.3: 7-19. Also available as Building research station current paper CP 12/75.

Coyle, H.M. and Reese, L.C. (1966) Load transfer for axially loaded piles in clay. Journal of the Soil Mechanics and Foundations Division (ASCE), **92**(2), 1-26.

Crispin J.J., Leahy, C.P. and Mylonakis, G. (2018). Winkler Model for Axially-Loaded Piles in Inhomogeneous Soil. (under review).

Deltares (2016) D-Pile Group User Manual – 3D modelling of simple pile and pile groups. Deltares. Available at: https://content.oss.deltares.nl/delft3d/manuals/DPileGroup-Manual.pdf, accessed 12th April 2018.

Fine (n.d.) Engineering manuals for GEO5 programs – part 2. Fine Ltd. Available at: http://geo5-software.de/de/support_files/projektierungshandbucher/geo5-engineering_manuals_em2.pdf, accessed 12th April 2018.

Fleming, W.G.K. (1992). A new method for single pile settlement prediction and analysis. Géotechnique, **42**(3), 411-425, https://doi.org/10.1680/geot.1992.42.3.411.

Fleming, W.G.K., Weltman, A.J., Randolph, M.F. and Elson, W.K. (2009). Piling Engineering, 3rd edn. Wiley, New York, NY, USA.

Galbraith, A.P., Farrell, E.R. and Byrne, J.J. (2014). Uncertainty in pile resistance from static load tests database. Proceedings of the Institution of Civil Engineers - Geotechnical Engineering, **167**(5), 431-446, https://doi.org/10.1680/geng.12.00132.

Guo W.D. (2012). Theory and Practice of Pile Foundations. CRC Press.

Koutsoftas, D. C., Karina, K. and Hashash, Y. M. A. (2017). Discussion of "Index Test Method for Estimating the Effective Preconsolidation Stress in Clay Deposits" by Karim Kootahi and Paul W. Mayne. Journal of Geotechnical and Geoenvironmental Engineering, American Society of Civil Engineers, 143(10), article no. 07017030, https://doi.org/10.1061/(ASCE)GT.1943-5606.0001764.

Kootahi, K. and Mayne, P. W. (2017). Closure to "Index Test Method for Estimating the Effective Preconsolidation Stress in Clay Deposits" by Karim Kootahi and Paul W. Mayne. Journal of Geotechnical and Geoenvironmental Engineering (ASCE), 143(10), article no. 07017031, https://doi.org/10.1061/(ASCE)GT.1943-5606.0001765.

LDSA: London District Surveyors Association (2009). Foundations no. 1: Guidance notes for the design of straight shafted bored piles in London clay. Bromley, UK.

Lemnitzer, A. and Favaretti, C. (2013). Find a Pile.com. Available at: http://www.findapile.com/, accessed 29th June 2018.

Mylonakis, G. and Gazetas, G. (1998). Settlement and additional internal forces of grouped piles in layered soil. Géotechnique, **48**(1), 55-72, https://doi.org/10.1680/geot.1998.48.1.55.

Mylonakis, G. (2001). Winkler modulus for axially loaded piles. Géotechnique, **51**(5), 455-461.

OASYS (2017) Pile Oasys Geo Suite for Windows. Available at: https://www.oasys-software.com/wp-content/uploads/2017/11/pile19.6_manual.pdf, accessed 29th June 2018.

Ottaviani, M. (1975). Three-dimensional finite element analysis of vertically loaded pile groups. Géotechnique, 25(2), 159-174, https://doi.org/10.1680/geot.1975.25.2.159.

Paikowsky S.G., Brigisson, B., McVay, M., Nguyen, T., Kuo, C., Baecher, G., Ayyub, B., Stenersen, K., O'Malley, K., Chernauskas, L. and O'Neill, M. (2004) Load and Resistance Factor Design (LRFD) for Deep Foundations. NCHRP Report 507, National Cooperative Highway Research Program, Transportation Research Board

Patel, D.C. (1989). A case study of the shaft friction of bored piles in London Clay in terms of total and effective stresses. MSc thesis, Imperial College London, UK.

Patel, D.C. (1992). Interpretation of results of pile tests in London clay. Piling Europe, Thomas Telford, London, UK.

Poulos, H.G. (1968). Analysis of the settlement of pile groups. Géotechnique **18**, 449-471.

Poulos, H.G. (1989). Pile behaviour – theory and application. Géotechnique, **39**(3), 365-415, https://doi.org/10.1680/geot.1989.39.3.365.

Poulos, H.G. (1999). Common procedures for foundation settlement analysis – are they adequate? Australian Geomechanics Journal, **34**(1), 13-38.

Poulos, H.G. and Davis, E.H. (1968). The settlement behaviour of singly axially loaded incompressible piles and piers. Géotechnique, **18**(3), 351-371, https://doi.org/10.1680/geot.1968.18.3.351.

Randolph, M.F. and Wroth, C.P. (1978). Analysis of deformation of vertically loaded piles. Journal of the Geotechnical Engineering Division, American Society of Civil Engineers, **104**(12), 1465-1488.

Randolph, M.F. and Wroth, C.P. (1979). Analysis of vertical deformation of pile groups. Géotechnique **29(**4), 423-439.

Randolph, M.F. (2003). Science and empiricism in pile foundation design. Géotechnique, **53**(10), 847-875, https://doi.org/10.1680/geot.2003.53.10.847.

Randolph, M.F. (2006) PIGLET – Analysis and design of pile groups. University of Western Australia, Crawley, Western Australia, Australia.

Reese, L.C., Wang, S.T. and Arrellaga, J.A. (2014) TZPILE 2014 user's manual - Analysis of load versus settlement for an axially-loaded deep foundation. ENSOFT INC. Austin, Texas, USA. Available at: https://www.ensoftinc.com/products/tzpile/doc/tzpile-users-manual.pdf, accessed 29th June 2018.

Scott R.F. (1981). Foundation Analysis. Prentice Hall.

Seed, H.B. and Reese, L.C. (1957). The action of soft clay along friction piles. Transactions of the American Society of Civil Engineers, **122**, 731-764.

Skempton, A.W. (1959). Cast-in-situ bored piles in London clay. Géotechnique, **9**(4), 153-173, https://doi.org/10.1680/geot.1959.9.4.153.

Syngros, K. (2004). Seismic Response of Piles and Pile-Supported Bridge Piers Evaluated Through Case Histories, PhD Thesis, The City College of the City University of New York, NY, USA.

Tomlinson, M. and Woodward, J. (2014). Pile design and construction in practice. 6th Edition, CRC Press, Boca Raton, FL, USA.

Vardanega, P. J. and Bolton, M. D. (2011a). Strength mobilization in clays and silts. Canadian Geotechnical Journal, **48**(10), 1485-1503, http://doi.org/10.1139/T11-052 and Corrigendum, **49**(5), 631, http://doi.org/10.1139/t2012-023

Vardanega, P. J. and Bolton, M. D. (2011b). Predicting Shear Strength Mobilisation of London Clay. Proceedings 15th European Conference on Soil Mechanics and Geotechnical Engineering: Geotechnics of Hard Soils – Weak Rocks, A. Anagnostopoulos et al. eds., IOS Press, Amsterdam, The Netherlands, vol. 1 pp. 487-492, http://doi.org/10.3233/978-1-60750-801-4-487

Vardanega, P.J., Williamson, M.G. and Bolton, M.D. (2012a). Bored pile design in stiff clay II: mechanisms and uncertainty. Proceedings of the Institution of Civil Engineers - Geotechnical Engineering, **165**(4), 233-246; https://doi.org/10.1680/geng.11.00063; Corrigendum, **166**(5), 518; https://doi.org/10.1680/geng.2013.166.5.518.

Vardanega, P.J., Kolody, E., Pennington, S.H., Morrison, P.R.J. and Simpson, B. (2012b). Bored pile design in stiff clay I: codes of practice. Proceedings of the Institution of Civil Engineers - Geotechnical Engineering, **165**(4), 213-232; https://doi.org/10.1680/geng.11.00062.

Vardanega, P.J., Crispin, J.J., Gilder, C.E.L., Voyagaki, E., Shepheard, C.J. and Holcombe, E.A. (2018). Geodatabases to Improve Geotechnical Design and Modelling. ce/papers, **2**(2-3), 401-406. https://doi.org/10.1002/cepa.704.

Whitaker, T. and Cooke, R.W. (1966). An investigation of the shaft and base resistance of large bored piles in London Clay. In: Large Bored Piles: Proceedings of the Symposium by the Institution of Civil Engineers and the Reinforced Concrete Association; Institution of Civil Engineers, London, UK, 7-49.

Yang, Z., Jardine, R., Guo, W. and Chow, F. (2015). A new and openly accessible database of tests on piles driven in sands. Géotechnique Letters, **5**(1), 12-20,

https://doi.org/10.1680/geolett.14.00075.
Yang, Z., Jardine, R., Guo, W. and Chow, F. (2016) A comprehensive database of tests on axially loaded piles driven in sand. Zhejiang University Press Co. Ltd. Published by Elsevier Inc.

TABLES

Table 1. Patel 1989, summary of pile tests presented in this study

Stats of Patel 1989 pile tests			
Site locations	15 sites in London	Pile diameters (*m*)	0.343-0.914
Number of test piles	51	Pile lengths (*m*)	6.1-24.2
Pile types	Bored, straight shafted & under reamed	Pile lengths in clay (*m*)	4.3-22.7
Test types	Maintained Load	Max head displacements (*mm*)	19.4
Geology	London Clay	Max applied load *(kN)*	3540

Table 2. Pile lengths in London Clay, *L,* and pile base diameters, D_b, normalised with pile shaft diameters, D_s, for the tests recorded in Patel 1989.

Site	Pile	L/D_s	D_b/D_s	Site	Pile	L/D_s	D_b/D_s
A1	TP1	17.1	1.0	A9	TP3	22.2	1.0
	TP2	25.4	1.0		TP4	28.9	1.0
A2	TP1	13.3	1.0		TP5	26.7	1.0
A3	TP1	11.7	1.0		TP6	20.0	1.0
A4	TP1	26.5	1.0	A10	P1	37.2	1.0
A5	TP1	14.0	1.0		P2	33.3	1.0
	TP2	16.8	2.8		P4	27.6	1.0
A6	24/7 10	22.0	1.0		P5	34.9	1.0
	29/2	16.0	1.0		P6	32.3	1.0
	95 4/25	14.9	1.0	A11	TP1	30.6	1.0
	B4	20.0	1.0		TP2	32.6	1.0
	B5	15.5	1.0	A12	TP1	13.5	2.3
	B6	15.0	1.0		TP2	15.0	1.0
	B7	11.5	1.0	A13	TP1	23.4	1.0
	B8	22.5	1.0		TP2	12.5	1.0
	B9	18.5	1.0	A14	4138	28.0	1.0
	B10	15.0	1.0		A	13.4	1.0
	B11i, ii	14.4	1.0		B	13.4	1.0
	B12	17.6	1.0		C	13.4	1.0
A7	TP1	16.9	1.0		TP1	30.0	1.0
	TP2	16.5	2.0		TP2	30.1	1.0
A8	TP1	30.3	1.0		TP3	26.7	1.0
	TP2	27.5	1.0	A15	TP1	20.0	1.0
A9	TP1	21.4	1.0		TP2	22.0	1.0
	TP2	17.8	1.0		TP3	15.0	1.0

Table 3. Applied and Predicted Loads

Site	Pile	Predicted Ultimate Load, P_u (kN)	Normalised Maximum Applied Test Load, P_{ML}/P_u	Normalised Load Prediction Range, P/P_u		
				Method 1	Method 2	Method 3
A1	TP1	445	0.90	0 -	0 - 1	0 - 0.73
	TP2	724	1.03	0 -	0 - 1	0 - 0.78
A2	TP1	517	0.67	0 -	0 - 1	0 - 0.70
A3	TP1	463	0.78	0 -	0 - 1	0 - 0.71
A4	TP1	1141	0.87	0 -	0 - 1	0 - 0.81
A5	TP1	783	0.93	0 -	0 - 1	0 - 0.73
	TP2	3999	0.73	0 -	0 - 1	0 - 0.67
A6	24/7 10	2156	0.67	0 -	0 - 1	0 - 0.73
	29/2	1871	0.67	0 -	0 - 1	0 - 0.70
	95 4/25	1716	0.67	0 -	0 - 1	0 - 0.69
	B4	1864	0.67	0 -	0 - 1	0 - 0.71
	B5	2235	0.67	0 -	0 - 1	0 - 0.73
	B6	1215	0.67	0 -	0 - 1	0 - 0.67
	B7	841	0.79	0 -	0 - 1	0 - 0.67
	B8	1277	0.76	0 -	0 - 1	0 - 0.67
	B9	1655	0.77	0 -	0 - 1	0 - 0.70
	B10	2134	0.67	0 -	0 - 1	0 - 0.71
	B11i	2907	0.67	0 -	0 - 1	0 - 0.68
	B11ii	2907	0.67	0 -	0 - 1	0 - 0.68
	B12	2875	0.67	0 -	0 - 1	0 - 0.68
A7	TP1	2789	0.67	0 -	0 - 1	0 - 0.72
	TP2	4961	0.67	0 -	0 - 1	0 - 0.67
A8	TP1	2147	0.71	0 -	0 - 1	0 - 0.81
	TP2	1865	0.80	0 -	0 - 1	0 - 0.79
A9	TP1	756	0.85	0 -	0 - 1	0 - 0.76
	TP2	601	0.75	0 -	0 - 1	0 - 0.74
	TP3	794	0.93	0 -	0 - 1	0 - 0.77
	TP4	1127	0.67	0 -	0 - 1	0 - 0.81
	TP5	1010	0.83	0 -	0 - 1	0 - 0.80
	TP6	695	0.86	0 -	0 - 1	0 - 0.75
A10	P1	4711	0.68	0 -	0 - 1	0 - 0.83
	P2	3976	0.67	0 -	0 - 1	0 - 0.81
	P4	3003	0.67	0 -	0 - 1	0 - 0.79
	P5	4269	0.75	0 -	0 - 1	0 - 0.82
	P6	3791	0.93	0 -	0 - 1	0 - 0.81
A11	TP1	980	1.22	0 -	0 - 1	0 - 0.77
	TP2	1103	1.09	0 -	0 - 1	0 - 0.78
A12	TP1	5428	0.67	0 -	0 - 1	0 - 0.67
	TP2	2673	0.73	0 -	0 - 1	0 - 0.71
A13	TP1	1797	0.67	0 -	0 - 1	0 - 0.78
	TP2	870	0.67	0 -	0 - 1	0 - 0.68
A14	4138	2419	0.74	0 -	0 - 1	0 - 0.78
	A	194	0.67	0 -	0 - 1	0 - 0.67
	B	194	0.72	0 -	0 - 1	0 - 0.67
	C	194	0.72	0 -	0 - 1	0 - 0.67
	TP1	2693	0.67	0 -	0 - 1	0 - 0.79

	TP2	1221	0.74	0 -	0 - 1	0 - 0.80
	TP3	1024	0.67	0 -	0 - 1	0 - 0.78
A15	TP1	3347	0.78	0 -	0 - 1	0 - 0.79
	TP2	2258	0.67	0 -	0 - 1	0 - 0.81
	TP3	1578	0.67	0 -	0 - 1	0 - 0.75

FIGURES

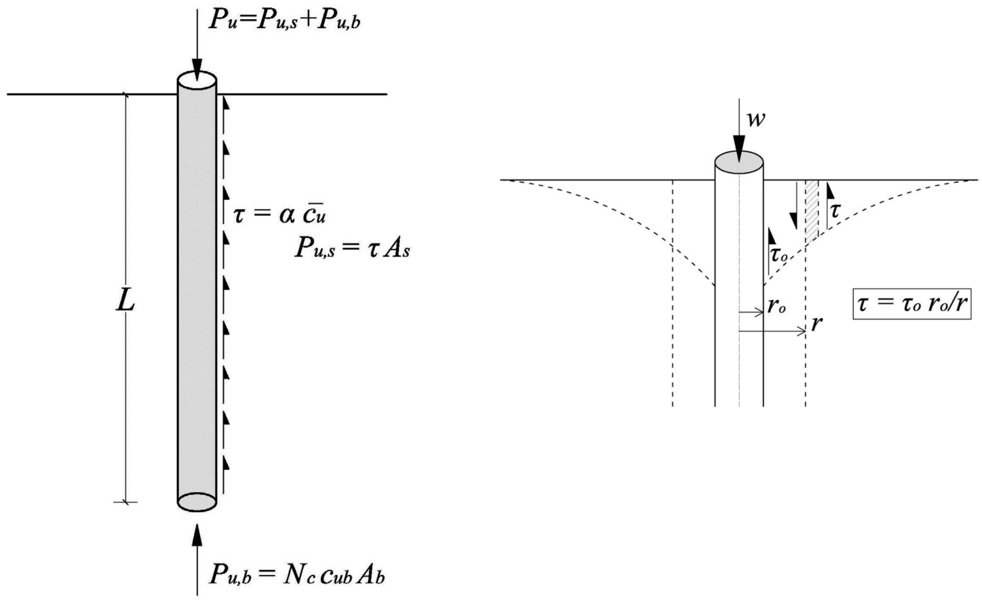

(a) (b)

FIG. 1. (a) Ultimate pile capacity distribution (*based on Skempton 1959*) and (b) displacement of a single pile *(based on Cooke 1974 and Randolph & Wroth 1978).*

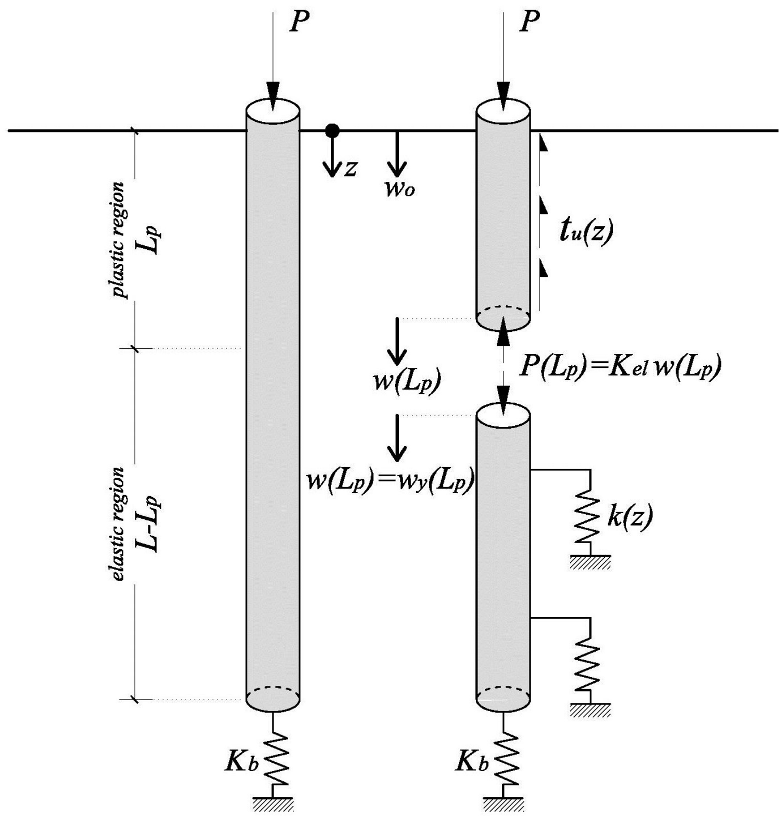

FIG. 2. Proposed Linear Elastic Perfectly – Plastic Model (Method 2) for a pile under axial load.

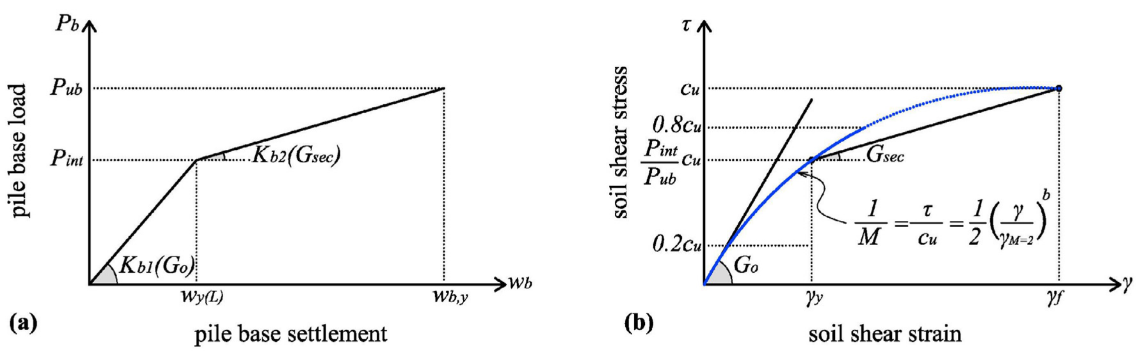

FIG. 3. (a) Bilinear base spring stiffness model; (b) Secant shear modulus, G_{sec}, estimation method.

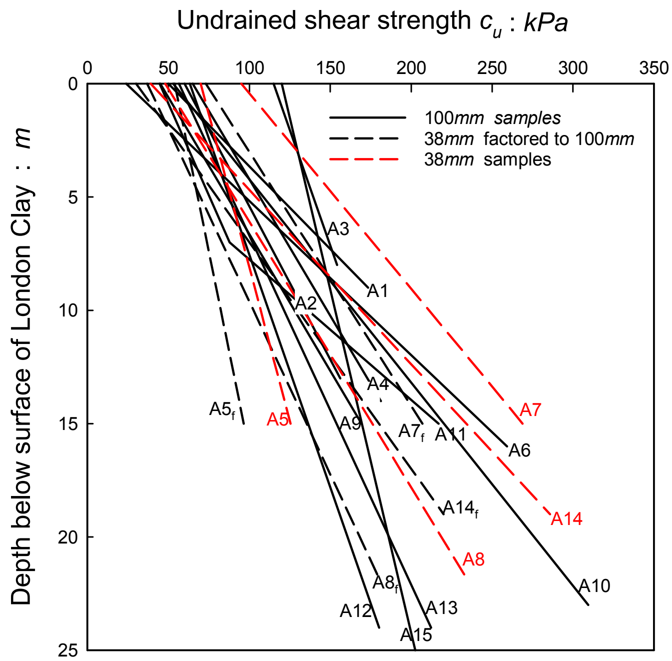

FIG 4. Undrained shear strength variation with depth for the reported sites in London Clay as determined from triaxial tests on 100*mm* and 38*mm* samples (*modified after Patel 1992*). Subscript *f* denotes factored profiles.

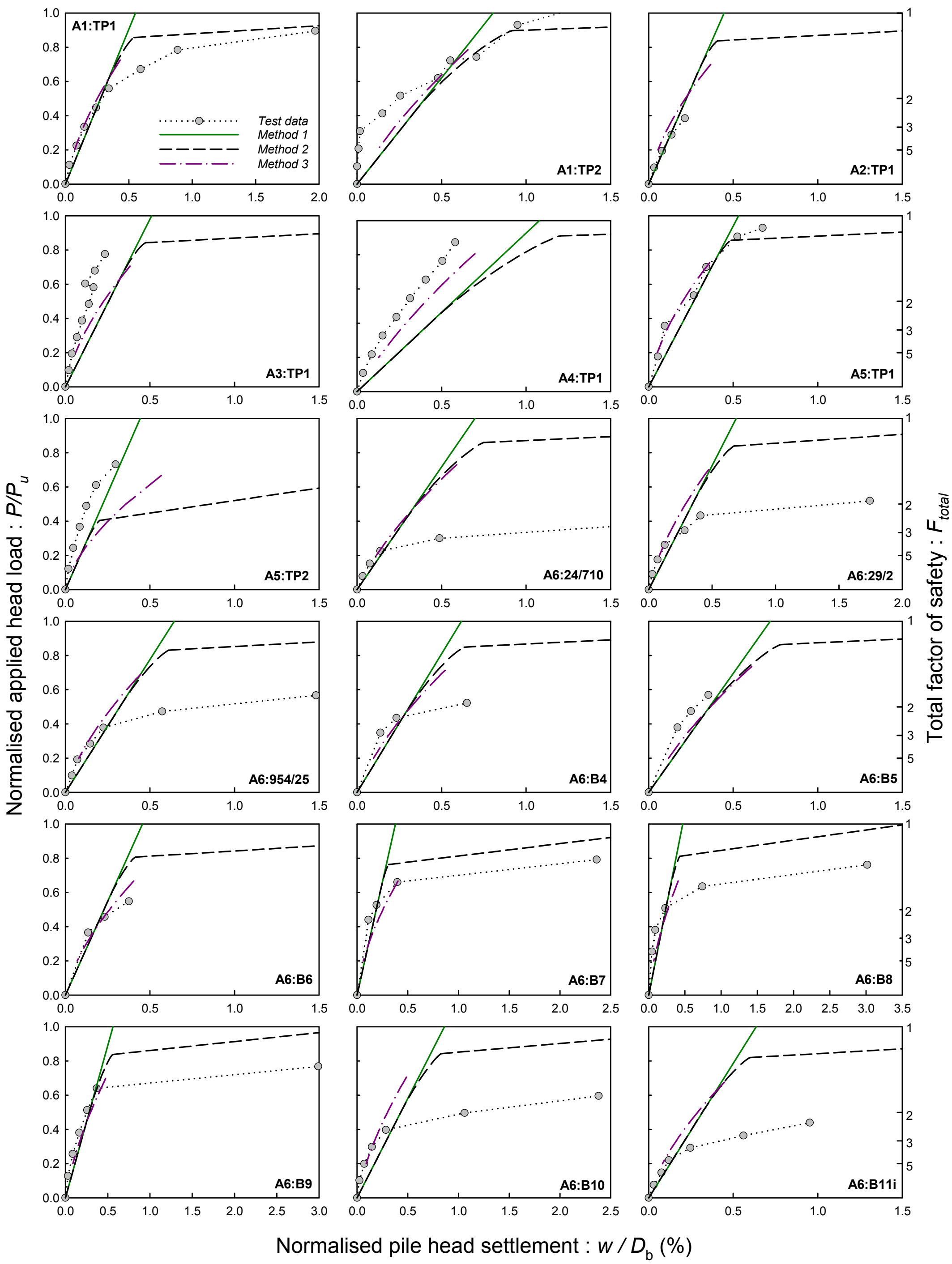

FIG. 5. Comparison of the predicted load–settlement curves using the three methods against the experimental results reported in Patel 1992. Method 1 (Crispin *et al.* 2018), Method 2 (Crispin *et al.* 2018), Method 3 (Vardanega *et al.* 2012a, 2018). (Test piles shown: A1/TP1 to A6/B11i).

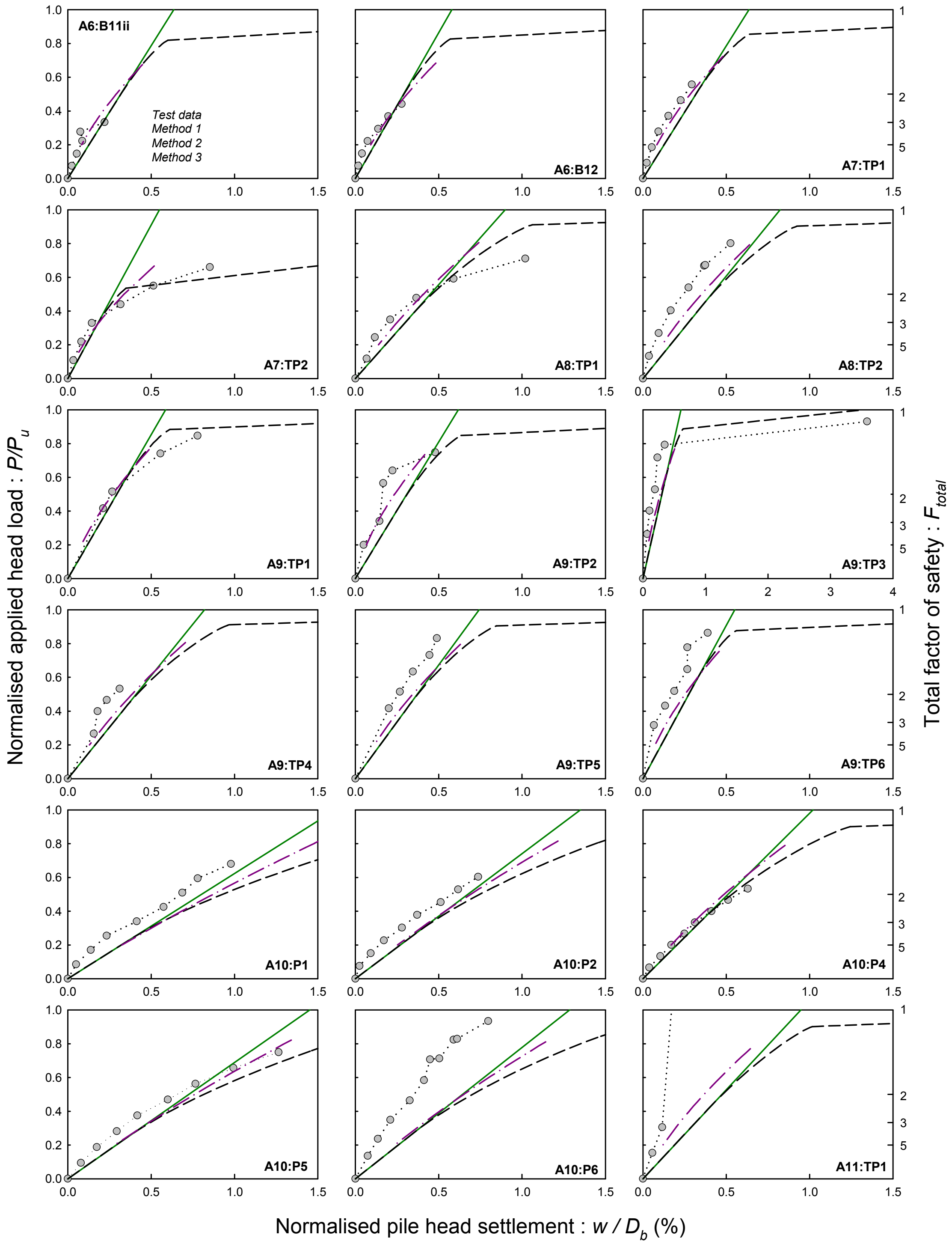

FIG. 6. Comparison of the predicted load–settlement curves using the three methods against the experimental results reported in Patel 1992. Method 1 (Crispin *et al*. 2018), Method 2 (Crispin *et al*. 2018), Method 3 (Vardanega *et al*. 2012a, 2018). (Test piles shown: A6/B11ii to A11/TP1).

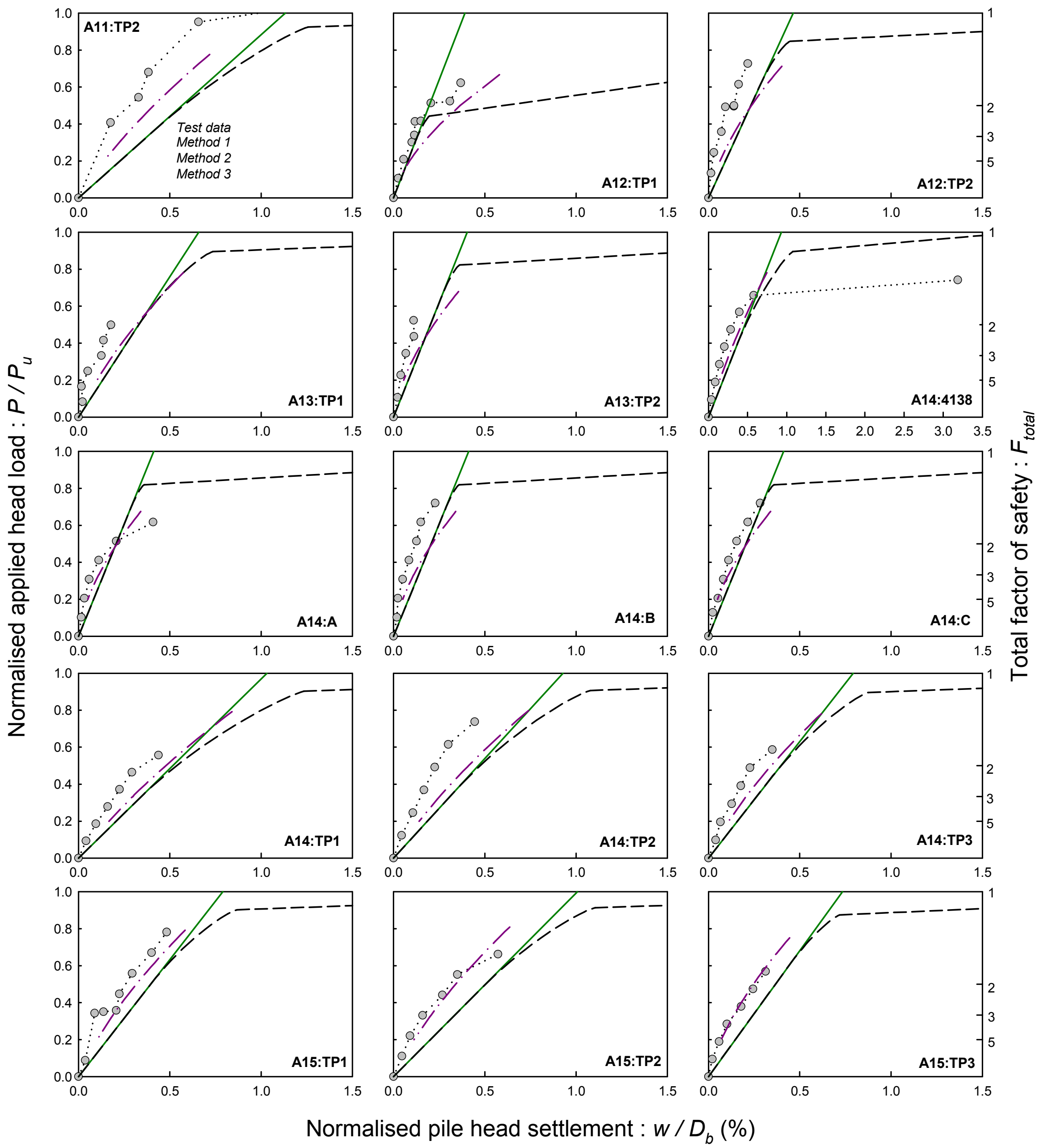

FIG. 7. Comparison of the predicted load–settlement curves using the three methods against the experimental results reported in Patel 1992. Method 1 (Crispin *et al*. 2018), Method 2 (Crispin *et al*. 2018), Method 3 (Vardanega *et al.* 2012a, 2018). (Test piles shown: A11/TP2 to A15/TP3).

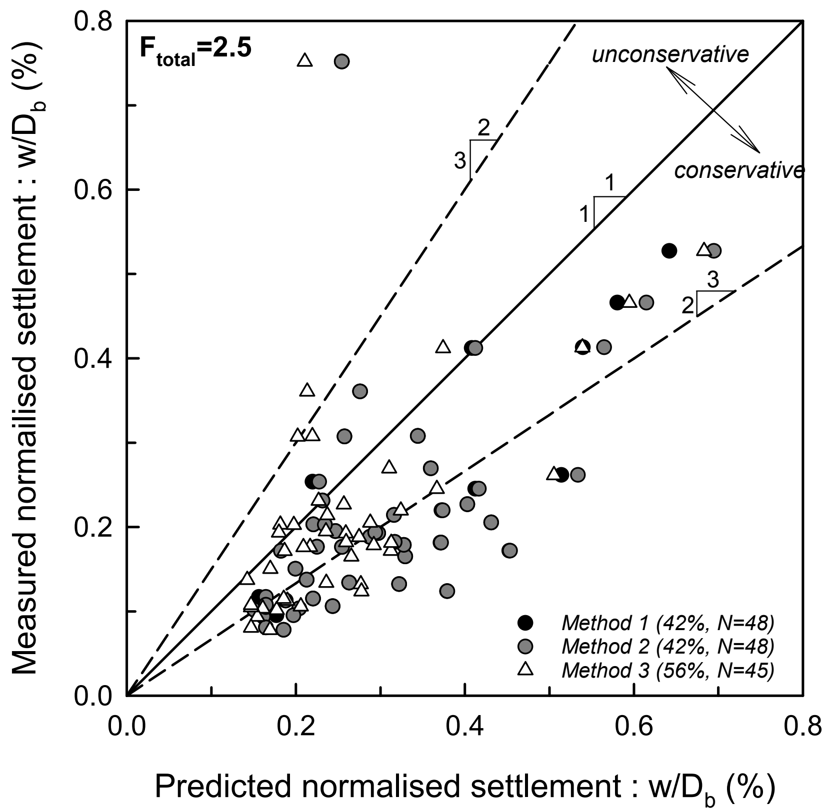

FIG. 8. Predicted vs. measured pile settlement *w,* normalised with pile base diameter D_b. Measured values for Patel 1992 test data. Predicted values generated by the three presented analytical approaches. Dashed lines represent ±50% prediction intervals. *N* denotes number of tests, loaded to that level, where methods apply. Percentages within the ±50% bounds are shown in parentheses in the legend. (Factor of safety F_{total}=2.5).

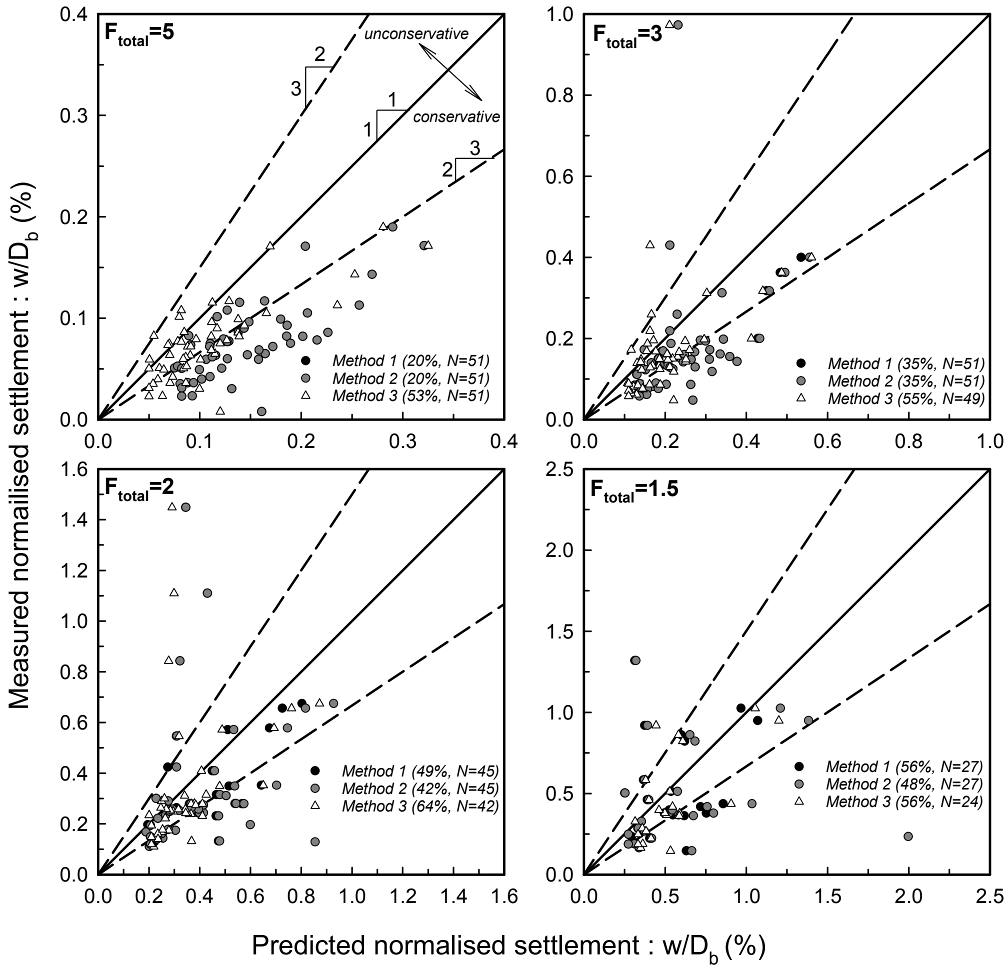

FIG. 9. Predicted vs. measured pile settlement *w*, normalised with pile base diameter D_b. Measured values for Patel 1992 test data. Predicted values by the three presented analytical approaches. Dashed lines represent ±50% prediction intervals. *N* denotes number of tests, loaded to that level, where methods apply. Percentages within the ±50% bounds are shown in parentheses in the legends.